

Test of statistical model predictions for alpha-particle decay of $^{90,92,94,96}\text{Ru}$ compound nuclei

B. Fornal,* F. Gramegna, and G. Prete

Istituto Nazionale di Fisica Nucleare, Laboratori Nazionali di Legnaro, I-36020 Legnaro (Padova), Italy

G. Nebbia and R. Smith

Istituto Nazionale di Fisica Nucleare and Dipartimento di Fisica dell'Università di Padova, I-35131 Padova, Italy

G. D'Erasmus, L. Fiore, A. Pantaleo, and G. Viesti

Istituto Nazionale di Fisica Nucleare and Dipartimento di Fisica dell'Università di Bari, I-70126 Bari, Italy

P. Blasi and F. Lucarelli

Istituto Nazionale di Fisica Nucleare and Dipartimento di Fisica dell'Università di Firenze, I-51025 Firenze, Italy

I. Iori and A. Moroni

Istituto Nazionale di Fisica Nucleare and Dipartimento di Fisica dell'Università di Milano, I-20133 Milano, Italy

(Received 31 May 1989)

The α decay of Ru compound nuclei populated in ^{32}S on $^{58,60,62,64}\text{Ni}$ reactions at $E_{\text{beam}} = 135\text{--}185$ MeV has been studied. Experimental data have been compared with statistical model calculations performed with two different computer codes. The quality of the agreement between calculations and experimental data was found, in one case, to depend on the compound nucleus populated. Comparing the results from the two computer codes, deviations in the predicted cross sections are evidenced which are due to the different parametrization of nuclear properties employed in the calculations. Statistical model calculations describe well the shape of experimental spectra if account is taken of changes in the phase space available to the decaying nucleus which are related to the onset of deformations at high spins. Fission competition strongly determines the alpha-particle cross sections at the higher bombarding energies which are systematically underestimated by the model calculations if transmission coefficients computed from optical model potentials are used.

I. INTRODUCTION

The decay of compound nuclei at moderate excitation energy ($E_x \sim 100$ MeV) and high spin has received a renewed interest in the past years.^{1,2} New detailed experimental data and sophisticated model calculation allow us to probe whether the foundations of the statistical model hold for compound nuclei (CN) populated in heavy ions reactions. Assuming that the statistical nature of the compound nucleus decay is experimentally ascertained, open questions are still related to the description of the average shapes of highly excited, rapidly rotating nuclei and their influences on the basic parameters of the calculation (yrast lines, level densities, and emission barriers).

Recently several papers have been devoted to these topics and the field is not yet free from controversies on the degree of deformation induced by nuclear rotation.³ The common procedure to identify signatures of deformation effects is the comparison between experimental observables (energy spectra, anisotropies, and decay branches) and the results of statistical model calculations which include nuclear structure information as it is known today, i.e., mainly for spherical and/or cold nuclei. A disagreement between experimental data and calculations is taken as a demonstration that deformation induced by high

spins sets in, is not destroyed by thermal fluctuations, and is not described properly by the current parametrizations of nuclear properties included in the statistical model calculations. Empirical variations of the phase space available to the decaying compound nucleus and of the access to this phase space, needed to reproduce the experimental data, are obtained by changing the yrast line and emission barriers, respectively. These variations are used to estimate the change of the nuclear properties.

Evidences of deformation effects have been derived in several cases.^{1,2} In particular we have studied in the past the decay of ^{59}Cu (Refs. 4–6) and ^{67}Ga (Ref. 7) compound nuclei by comparing experimental data with statistical model calculations using the computer code CASCADE.⁸ In both cases it was found that the shape of the alpha-particle spectra is reproduced by model calculations in which the changes in yrast line and emission barriers result in a reduction of the emission from high spin states in the first decay step.

We present here data on the alpha-particle decay from $^{90,92,94,96}\text{Ru}$ compound nuclei populated at excitation energies in the range $E_x = 60\text{--}115$ MeV and spin up to $\sim 70\hbar$ by means of the reactions $^{32}\text{S} + ^{58,60,62,64}\text{Ni}$ at bombarding energies $E = 135\text{--}185$ MeV. Energy spectra and anisotropies of evaporative alpha particles have been

measured and compared with statistical model calculations using the computer codes CASCADE and PACE2.⁹

The experiment was performed to extend the investigation of the deformation effects in the mass region $A \sim 100$. Increasing the compound nucleus mass with respect to previous studies has the advantage of using statistical calculations in a region where the statistical models are expected to work well. Furthermore, in this mass region it is possible to describe the fission channel of the compound nucleus decay on the basis of experimental data, so that possible effects related to the opening of this channel on the evaporative alpha-particle spectra can be studied. The investigation of four compound nuclei offers the opportunity of testing the model calculation and the presence of deformation effects in a more systematic way.

II. EXPERIMENTAL DETAILS

The experiment was performed at the XTU Tandem facility of the Laboratori Nazionali di Legnaro. The ^{32}S

TABLE I. Fusion of ^{32}S on Ni isotopes studied in this work.

Reaction	E_{beam} (MeV)	E_x (MeV)	J_{crit}^a (\hbar)
$^{32}\text{S} + ^{58}\text{Ni}$	135–185	63.5–95.8	49–65
$^{32}\text{S} + ^{60}\text{Ni}$	135–185	71.0–103.7	50–67
$^{32}\text{Si} + ^{62}\text{Ni}$	135–185	77.8–110.9	51–69
$^{32}\text{S} + ^{64}\text{Ni}$	135–185	82.2–115.7	53–71

^aFrom cross sections of ^{32}S - and ^{35}Cl -induced reactions (Refs. 10 and 11) on Ni isotopes and systematics of reaction parameters (Ref. 12).

beam was focused onto thin (0.2–0.4 mg/cm²) foils of $^{58,60,62,64}\text{Ni}$, more than 96% enriched. The beam energy was varied from 135 to 185 MeV in 5 MeV steps. The corresponding excitation energies and spin region populated in the Ru compound nuclei are reported in Table I.

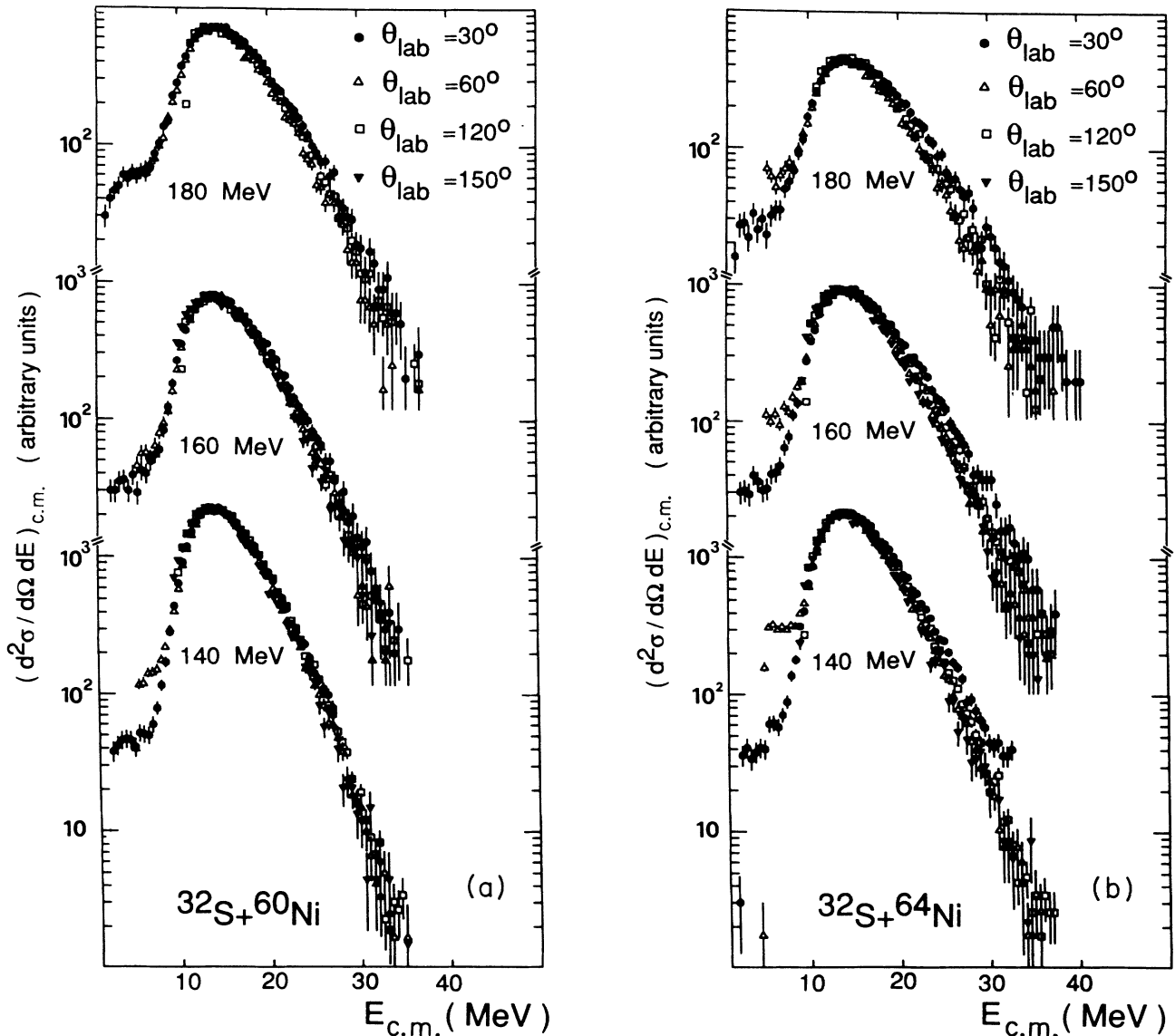


FIG. 1. Center-of-mass converted alpha-particle spectra taken at $\theta_{\text{lab}} = 30^\circ, 60^\circ, 120^\circ,$ and 150° for the reaction $^{32}\text{S} + ^{60}\text{Ni}$ (a) and $^{32}\text{S} + ^{64}\text{Ni}$ (b) at $E = 140, 160,$ and 180 MeV bombarding energies.

Spectra of alpha particles were collected at laboratory angles $\theta_{\text{lab}} = 30^\circ, 60^\circ, 120^\circ,$ and 150° using four silicon telescopes ($\Delta E = 10\text{--}20 \mu\text{m}, E = 1000\text{--}2000 \mu\text{m}$). Absolute cross section normalization was derived by calibrating the Faraday cup to the Rutherford scattering from a gold target. Energy calibrations were obtained by means of radioactive sources and precision pulsers.

In the bombarding energy range here explored the inclusive light particle spectra are largely dominated by the emission from the compound nucleus.^{3,6,7} To verify the evaporative origin of the alpha particles, energy spectra taken at different angles were converted to the center-of-mass (c.m.) system and compared with each other. In Fig. 1 examples are shown of c.m. converted energy spectra for $^{60,64}\text{Ni}$ targets. It is clearly seen that the low energy part and the peak in the energy spectra do not change with the observation angle. The spectra taken at $\theta_{\text{lab}} = 30^\circ$ with ^{64}Ni are characterized by a slope giving an apparent temperature slightly larger than that corresponding to other observation angles. This feature becomes more evident at increasing bombarding energy and is also present with ^{58}Ni target. In rapidly rotating nuclei the mean energy of the evaporated particles is expected to increase with average spin of the emitter, which is in turn related to the emission angle.¹³ A dependence of the observed slope with the observation angle might be explained as a spin effect. This seems not to be the case of the present experiment because this effect is present only for the reactions on $^{58,64}\text{Ni}$ but not for those on $^{60,62}\text{Ni}$ and is seen only at $\theta_{\text{lab}} = 30^\circ$ and not in the spectra taken at $\theta_{\text{lab}} = 150^\circ$, which corresponds to particles emitted even closer to the beam direction in the c.m. system. The

dependence on the bombarding energy and on the target supports the hypothesis that the extra production of more energetic particles is due to the sequential decay from projectile-like fragments after deep inelastic collisions, $\theta_{\text{lab}} = 30^\circ$ being close to the grazing angle of these reactions. In case of two-body reaction, the correlated angle for the target-like recoil is in the range $\theta_{\text{lab}} = 50^\circ\text{--}70^\circ$. The spectra taken at $\theta_{\text{lab}} = 60^\circ$ show a small rise at very low energies in case of ^{64}Bi target which can be explained as due to the corresponding sequential decay from the target-like fragment. We stress that the contamination from other reactions, if any, is very weak and the slope of the spectra taken at angles larger than $\theta_{\text{lab}} = 30^\circ$ fit nicely with each other, a proof that the source of the alpha particle is in these cases the compound nucleus.

III. EVAPORATION CALCULATIONS

Statistical model calculations have been performed using the computer codes CASCADE and PACE2. Input parameters are reported in Tables II and III for CASCADE and PACE2, respectively. Both codes perform multistep calculations (i.e., they follow step by step the decay of the CN allowing fission decay, particles, and gamma emission until the system cools down). CASCADE employs the grid method, mapping the evaporation residue in the $E_x\text{--}J$ plane and performing successive statistical calculations for any $E_x\text{--}J$ state until all reaction products fall below the thresholds for particle emission. CASCADE outputs the evaporation residue (ER) distributions, c.m. energy

TABLE II. Evaporation calculations using CASCADE.

Angular momentum distribution in the compound nucleus:
1. J_{max} derived from systematics of σ_{fus} .
2. Diffuseness $\Delta = 2\hbar$.
Myers-Swiiatecki Lysekil liquid-drop mass formula (Ref. 14).
Optical potential for emitted particles:
1. Neutrons, Wilmore and Hodgson (Ref. 15).
2. Protons, Perey (Ref. 16).
3. α particles, Huizenga and Igo (Ref. 17).
Level density parameters at low excitation ($E^* \leq 10$ MeV):
1. Fermi gas level density formula (Ref. 18) with empirical parameters from Dilg. ¹⁹
2. Effective moment of inertia $\mathcal{I} = 0.85 \times \mathcal{I}_{\text{rigid}}$:
Level density parameters at high excitation ($E^* \geq 15$ MeV):
1. Fermi gas level density formula (Ref. 18) with parameters from liquid-drop model (LDM) (Ref. 20).
2. Level density parameter $a_{\text{LDM}} = A/8.5 \text{ MeV}^{-1}$
Yrast line:
1. Moment of inertia for rigid body with radius parameter $r_0 = 1.28$ fm.
2. Deformability parameters (DEF and DEFS) used to calculate the effective moment of inertia
$\mathcal{I} = \mathcal{I}_{\text{sphere}} \times (1 + \text{DEF} \times J^2 + \text{DEFS} \times J^4)$,
as a function of the angular momentum J :
set 1 and set 2: $\text{DEF} = 0.15 \times 10^{-5}$, $\text{DEFS} = 0.16 \times 10^{-7}$,
Fission:
1. Level density parameter at the saddle point $a_f = A/\text{DAF} \text{ MeV}^{-1}$:
set 1: $\text{DAF} = 8.5$; set 2 and set 3: $\text{DAF} = 8.17$.
2. Fraction of the liquid-drop fission barrier ²¹ FFB:
set 1: $\text{FFB} = 1.0$; set 2 and set 3: $\text{FFB} = 0.54$.

TABLE III. Evaporation calculations using PACE2.

Angular momentum distribution in the compound nucleus:
1. J_{\max} derived from systematics of σ_{fus} .
2. Diffuseness $\Delta = 2\hbar$.
Wapstra mass (Ref. 22).
Optical potential for emitted particles:
SUBROUTINE TCCAL, E. D. Arthur, LASL Group T2.
Level density
Gilbert-Cameron level densities (Ref. 23) with parameter $a = A/8.5$ MeV.
Yrast line and fission barrier:
SUBROUTINE BARFIT, A. J. Sierk, LANL, Group T9, 1984 (Ref. 24).

spectra of the emitted particles, and cross sections for particles as well as for gamma and fission decay. The PACE2 code makes use of the Monte Carlo method, following the cooling down of the CN event by event and constructing the spectra in the c.m. as well as in the laboratory system. The simulation statistics in the PACE2 version here used is limited to a maximum of 10 000 events. As a result energy spectra often suffer from low statistics. The PACE2 code uses the same transmission coefficients T_l for all compound nuclei on the deexcitation path, taking into account an average reduction of the Coulomb barrier due to the evaporation. The CASCADE code, instead, computes T_l for any emitter taking part to the decay chain.

The first step in the statistical calculations for the Ru compound nuclei is related to the description of the fission channel. From the experimental point of view it is known that fission of the compound nucleus is an important decay channel for systems like the ones considered in this work.²⁵

PACE2 contains up-to-date evaluation of angular-momentum-dependent fission barriers,²⁴ while CASCADE includes the fission subroutine written for the code ALICE with original rotating liquid-drop model (RLDM) barriers.²¹ In Ref. 25 it has been shown that for the system $^{35}\text{Cl} + ^{62}\text{Ni}$, close to the ones studied here, a consistent reduction of the RLDM barrier and an increase of the level density at the saddle point relative to that of the rotating ground state (a_f/a_v) are needed to reproduce the experimental fission data. Blann and Komoto²⁶ have shown that the corrections needed to the RLDM fission barrier are correlated to the trend of those calculated by Krappe, Nix, and Sierk with the finite range model.²⁷

To test the fission channel predictions, we have performed cross section calculations for the $^{35}\text{Cl} + ^{62}\text{Ni}$ system using PACE2, CASCADE with default options (original RLDM barriers and $a_f/a_v = 1$), and CASCADE with adjusted fission parameters following Ref. 25 (RLDM barriers reduced by a factor 0.54 and $a_f/a_v = 1.04$). The results are shown in Fig. 2. It appears that the default CASCADE calculations underestimate largely the fission cross section for bombarding energies below $E = 200$ MeV. Appropriate estimates are obtained by the default PACE2 or adjusted CASCADE calculations.

Statistical model calculations for the decay of Ru compound nuclei were performed using PACE2 with default

options, CASCADE with default parameters (set 1 input in the following) and CASCADE with adjusted fission parameters (set 2 input). The two different CASCADE calculations were performed in the attempt of studying the influence of the fission channel on the calculated particle spectra. The comparison between experiment and calculations was performed in the center-of-mass system by using directly the experimental spectra taken at $\theta_{\text{lab}} = 60^\circ$ converted in the center-of-mass system assuming full

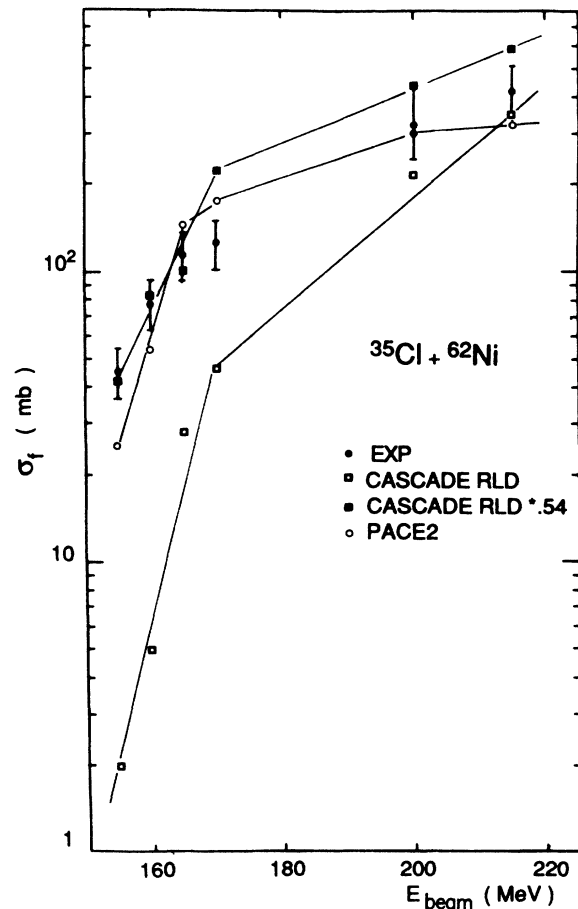


FIG. 2. Experimental²¹ and calculated fission cross section for the reaction $^{35}\text{Cl} + ^{62}\text{Ni}$. For details of calculations see the text.

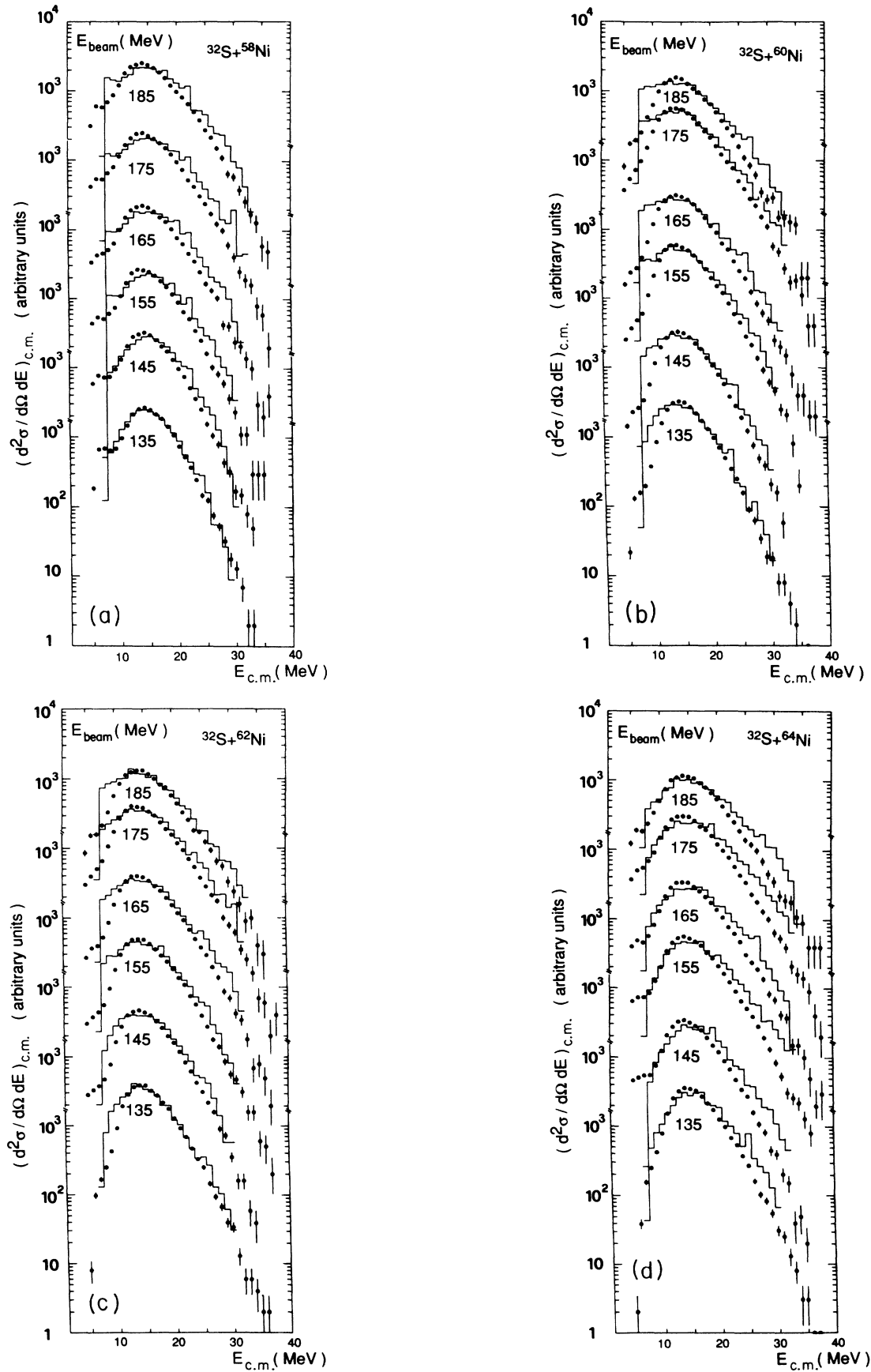


FIG. 3. Experimental and calculated alpha-particle spectra at $\theta_{lab} = 60^\circ$ for 135–185 MeV ^{32}S on ^{58}Ni (a), ^{60}Ni (b), ^{62}Ni (c), and ^{64}Ni (d). Statistical model calculations (histograms) are from the PACE2 code.

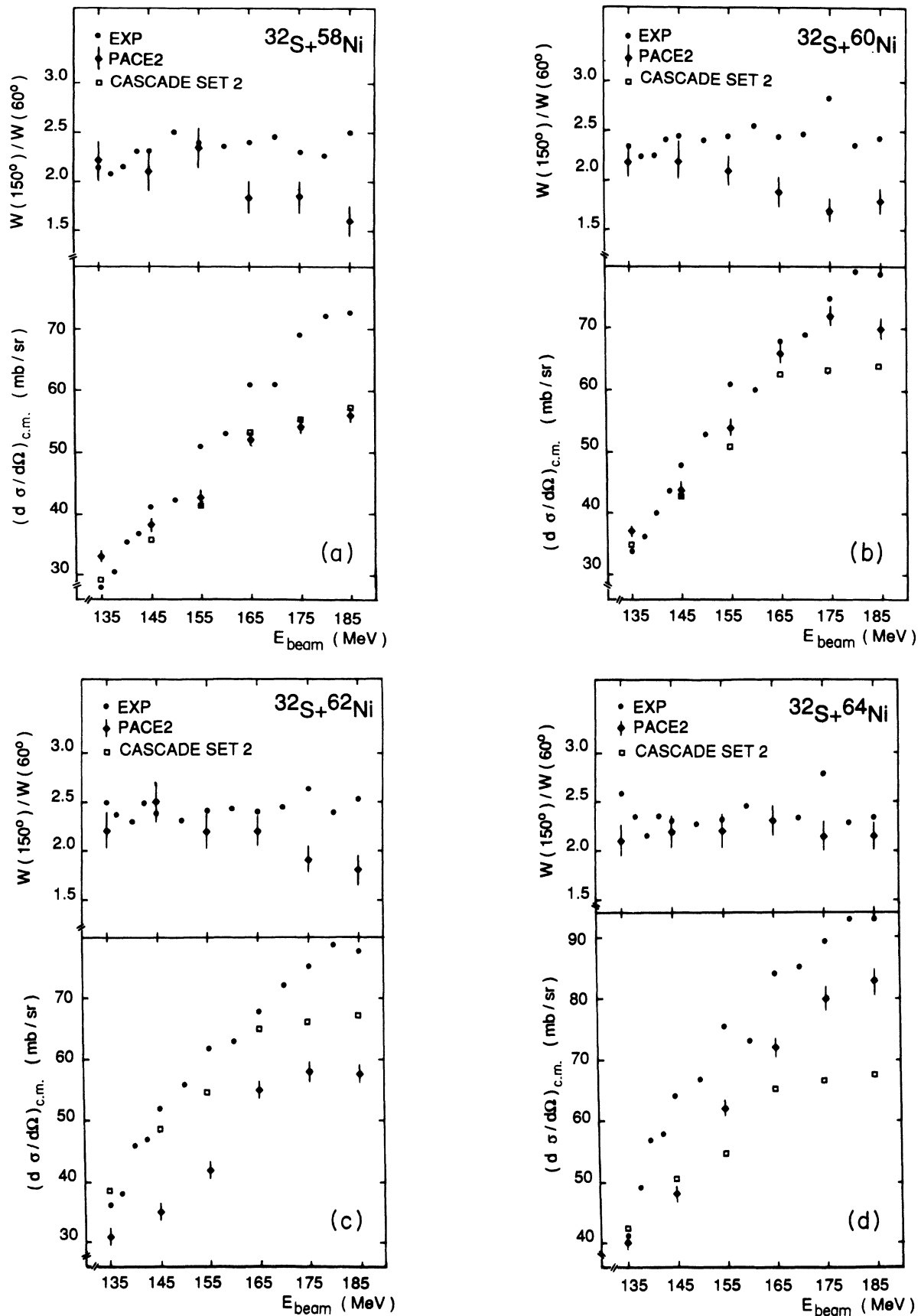


FIG. 4. Experimental and calculated cross sections at $\theta_{\text{lab}}=60^\circ$ and anisotropies for alpha-particle emission from 135–185 MeV ^{32}S on ^{58}Ni (a), ^{60}Ni (b), ^{62}Ni (c), and ^{64}Ni (d).

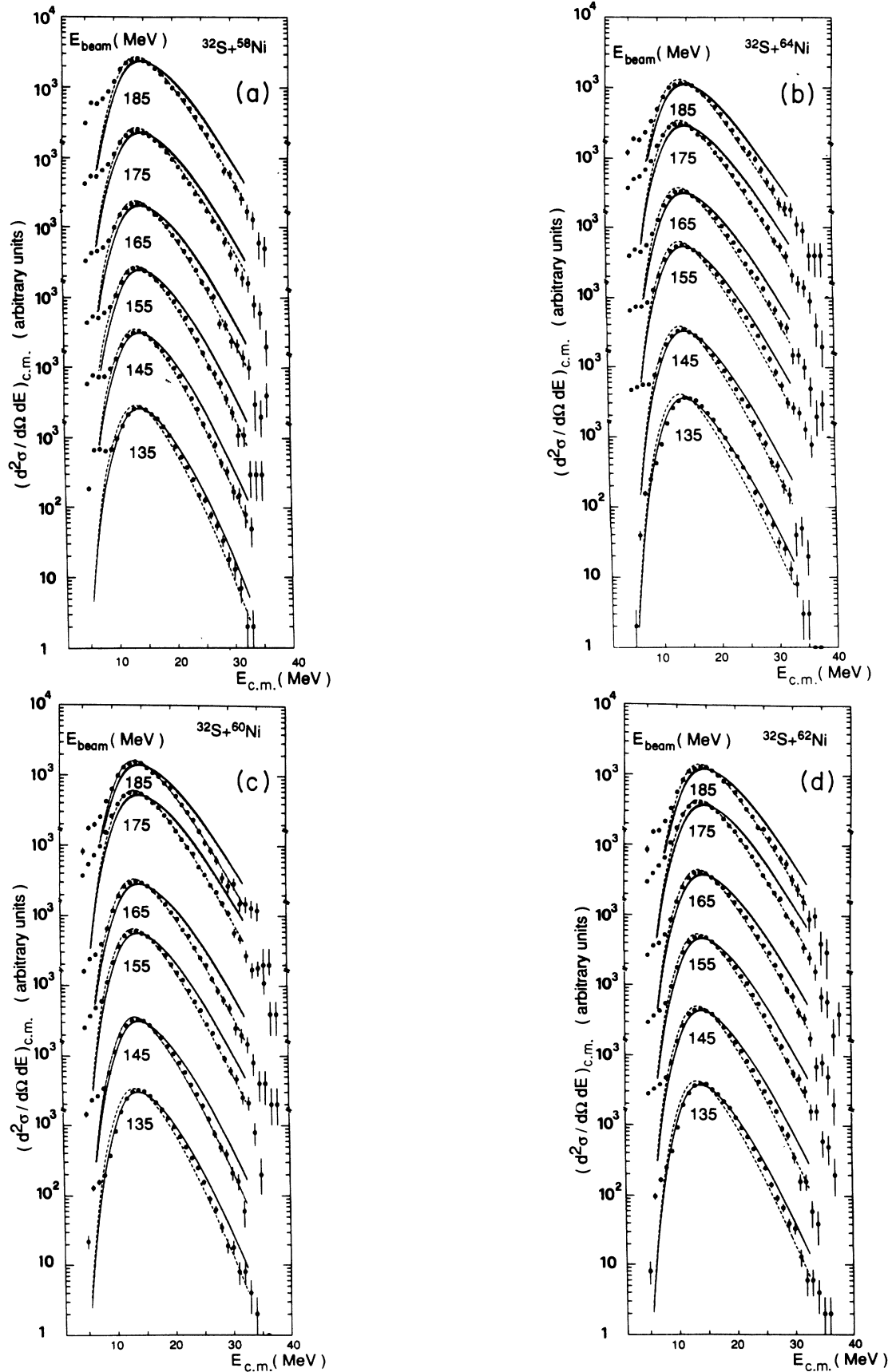


FIG. 5. As Fig. 3 but statistical model calculations are from the CASCADE code using different input parameters: set 1, solid line; set 2, dash-dotted line; set 3, dashed line. Note that differences between set 1 and set 2 calculations are evident only at the highest bombarding energy.

momentum transfer.

Figure 3 shows the prediction of PACE2 in terms of shape of alpha-particle spectra as compared with the experimental data. To better compare the spectral shapes, the calculated spectra have been normalized to the integral of the experimental distributions separately at each energy and for each isotope. In Fig. 4 we report a comparison of absolute cross sections at $\theta_{\text{lab}} = 60^\circ$ and anisotropies $W(150^\circ)/W(60^\circ)$ for alpha-particle emission.

In the range of targets, excitation energies, and angular momenta explored here, deviations appear between calculations and experiment which show a strong dependence on the compound nucleus. The PACE2 code describes well the shape of the alpha-particle spectra only at low bombarding energies ($E = 135\text{--}145$ MeV) for the ^{58}Ni target. At increasing bombarding energy, calculated spectra are wider than experimental ones and feature excess alpha particles at high as well as at very low energies. Excess low-energy alpha particles are present in the calculated spectra for the $^{60,62}\text{Ni}$ targets still at low bombarding energies.

In addition, neither absolute cross sections nor anisotropies are described well. In fact the calculated excita-

tion functions fit the data well only for the ^{60}Ni target. In the case of $^{62,64}\text{Ni}$ the calculated cross sections are $\sim 20\%$ lower than the experimental data. Calculated excitation functions flatten more rapidly than experimental ones for $^{58,62}\text{Ni}$. Calculated anisotropies reproduce well the experimental data at low bombarding energies for all targets, becoming somewhat lower than the experimental ones with increasing energy for $^{58,60,62}\text{Ni}$. In the case of ^{64}Ni the calculated anisotropies remain constant with the energy in agreement with the experimental data. In model calculations^{2,13} the calculated anisotropy is determined primarily by the ratio of the rotational energy to the temperature of the decaying system. In the single step calculation² of Ref. 2, predicted anisotropies for spherical nuclei are larger than the experimental data. This was taken as an evidence for deformation effects. In a multistep calculation the resulting anisotropy depends on the average spin and excitation energy of the states which populate the alpha channel. The fact that in the present case the calculated anisotropies underestimate the data cannot be taken as proof of the onset of deformation effects. This seems to offer a further demonstration that the PACE2 simulations do not correctly account for the CN

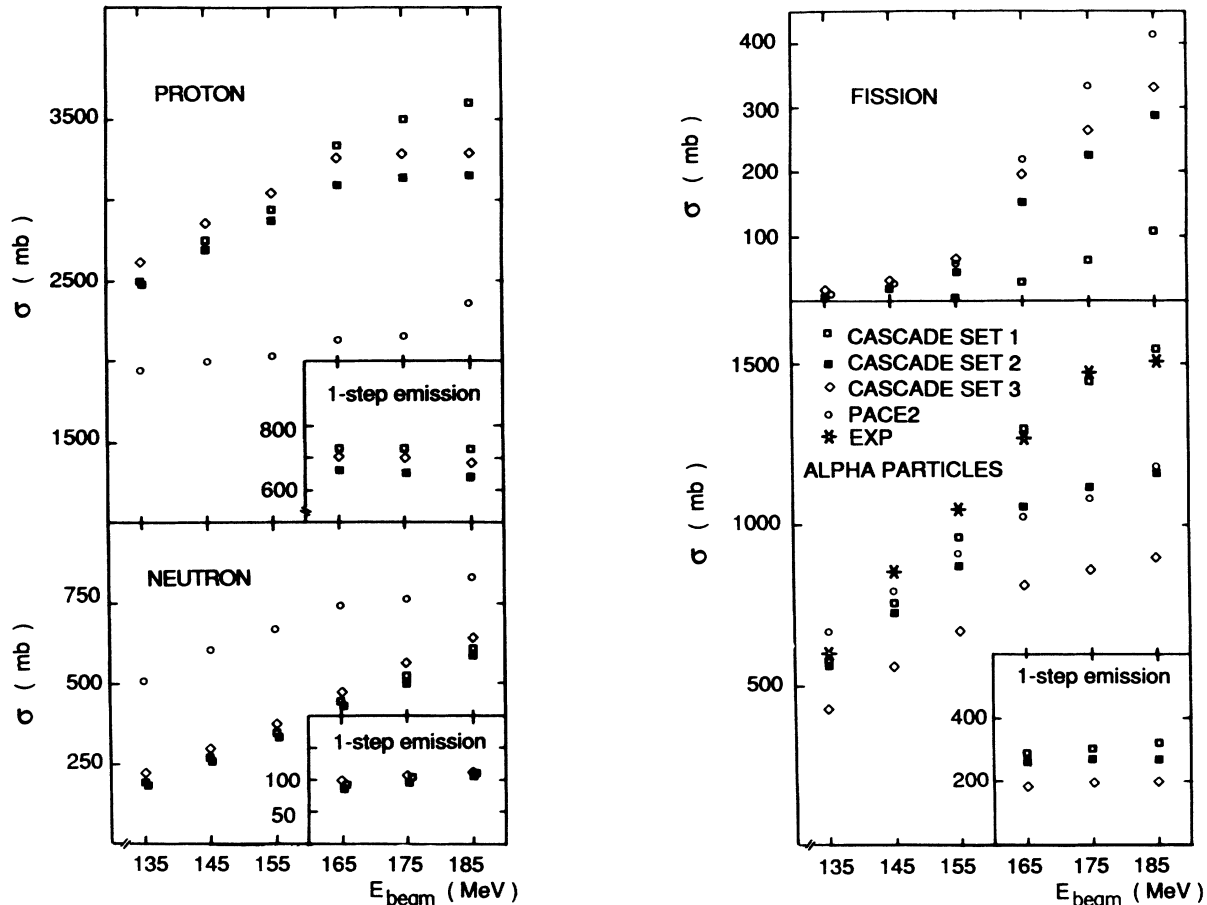


FIG. 6. Comparison of the cross sections for n , p (a), alpha emission and fission (b) for the $^{32}\text{S}+^{58}\text{Ni}$ reaction calculated from PACE2 and CASCADE using different input parameters. Experimental data for alpha emission obtained by angular integration of the measured spectra are also reported. Cross sections for emission in the first step of the decay chain are shown in the insets.

states which decay emitting alpha particles in the higher bombarding energies.

The PACE2 code allows a traceback of the CN decay thanks to the Monte Carlo technique. Considering for example the reactions at 185 MeV, the predictions are that alpha particles carry away, on the average, $E \sim 15$ MeV and sizeable angular momenta $l \sim 9\hbar$ and are emitted at any step of the deexcitation cascade. Only a small fraction of alpha particles originates in the first decay step (10–20%). The average angular momenta of the states which decay by alpha-particle emission are 5–10 \hbar lower than the average CN spin so that only 20% of alpha particles are emitted from states with RLDM predicted²⁸ shapes for which the ratio of the major axis to the spherical radius is $R_{\max}/R_0 \geq 1.1$.

Figure 5 shows the comparison between experimental spectra and the CASCADE predictions using the two sets of input parameters. The same normalization procedure used for Fig. 3 holds for Fig. 5. The first surprising feature of Fig. 5 is that the tuning of the fission channel achieved with the set 2 input parameters does not influence the shapes of the calculated alpha spectra which are identical to those calculated with set 1. CASCADE predictions are in good agreement with experimental spectra at low bombarding energy. An increasing deviation between calculation and experiment is evident with increasing bombarding energy. The calculations appear to underestimate the production of low-energy alpha particles and overestimate the yield of energetic ones. This results in a shift of the calculated spectra towards higher energies. For sake of comparison, we have computed from the integrated cross sections predicted by CASCADE (set 2 input) the differential cross sections at $\theta_{\text{lab}} = 60^\circ$ using experimental anisotropies. The results are shown in Fig. 4. The CASCADE excitation functions exhibit a saturation around $E = 165$ MeV not seen in the experimental data. For lower energies absolute cross sections are well reproduced with the only exception of the ^{64}Ni case. We stress the fact that the quality of agreement between CASCADE calculations and experimental data do not show the compound nucleus dependence which strongly appears in the case of PACE2 predictions. Comparing the spectra computed by CASCADE and PACE2 we note that the main difference is in the low-energy part of the distributions especially for $^{60,62}\text{Ni}$, the excess of energetic particles at the higher bombarding energies being present in the output of both codes and for all targets.

A more detailed comparison between the statistical model calculations is presented in Fig. 6 in the case of $^{32}\text{S} + ^{58}\text{Ni}$. It appears clearly that switching from set 1 to set 2 the CASCADE calculations approach the PACE2 ones in terms of fission and alpha-particle cross sections. At the higher bombarding energies the fission cross section calculated by PACE2 is still greater than that from CASCADE also with the set 2 input. More striking differences between the two codes are in the evaluation of the cross section for proton and neutron decay.

IV. DISCUSSION

In previous works^{5–7} on the decay of lighter compound nuclei it has been shown that the deviation be-

tween experimental alpha-particle spectra and predictions by the statistical model are related to the onset of deformations driven by the angular momenta. In the present work, as in the case of ^{59}Cu ,^{5,6} the increase of the average compound nucleus angular momentum is achieved by raising the bombarding energy. A representative yrast plot for the reaction studied here is reported in Fig. 7 where RLDM predictions are also reported on the nuclear deformation as a function of the angular momentum. It appears that at 135 MeV bombarding energy the bulk of the compound nucleus population is due to spherical or nearly spherical shapes. Sizable deformations ($R_{\max}/R_0 \geq 1.1$) are present only for spin $J \geq 45\hbar$. The relative population of deformed states increases with increasing bombarding energy up to $E = 185$ MeV. At this energy the CN spin distribution reaches the angular momentum value for which the fission barrier vanishes. It is assumed that the deviations between experimental spectra and calculations are caused by states in the angu-

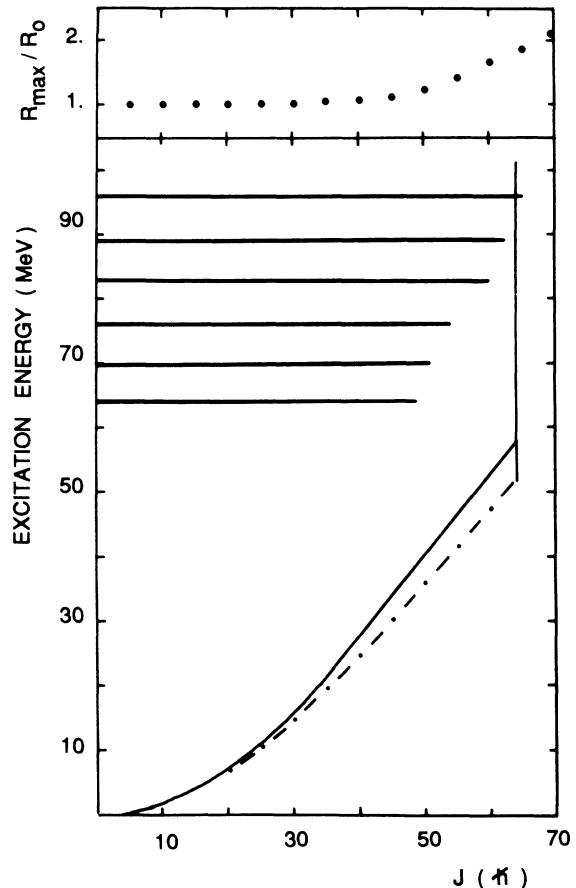


FIG. 7. Yrast plot for ^{90}Ru . Yrast lines are shown following set 1 and set 3 input data for statistical model calculations using the CASCADE code. The heavy horizontal lines indicate the angular momentum range and excitation energies associated with the fusion reactions studied in this work. The vertical line marks the angular momentum value for the vanish of the fission barrier. In the upper part are shown predictions from the RLDM for ratio of the major axis of the deformed compound nucleus to the spherical radius.

lar momentum window $45\hbar < J \leq 64\hbar$ which survive the fission decay, emitting alpha particles.

The effects of deformation on the spectra calculated from the statistical model code CASCADE are fully discussed in Ref. 6. The main phase space changes needed in the calculation for lighter CN to reproduce the experimental spectra are (i) a spin-dependent enhancement of the level density obtained by lowering the yrast line which decreases the extra production of energetic alpha particles from the first decay step, and (ii) the lowering of the emission barrier, achieved by increasing the optical model potential radius, which produces an amplification factor in the alpha-particle spectra determining the absolute cross section and favouring the emission of low-energy particles. These changes propagate on a complicated decay pattern constituted by many decay steps and their effects become evident only in the summed evaporation spectra at the end of the decay chain.

A further question is related to the differences between the predictions of the two codes, which appear in the present case to be sizable, especially for low-energy alpha particles. We have compared the yrast lines and transmission coefficients used in the calculations. The Sierk yrast line used in PACE2 is very close to the RLDM line used in CASCADE. Transmission coefficients for p , n , and alpha emission used in the two codes are also similar: At the top of the decay chain, the barriers for protons and alpha particles emitted at $l=0$ in CASCADE are $B_{l=0}^p=8.5$ MeV and $B_{l=0}^\alpha=12.1$ MeV to be compared with the values $B_{l=0}^p=7.8$ MeV and $B_{l=0}^\alpha=12.7$ MeV used as average values in PACE2. In both statistical model codes, the T_l are computed from parametrizations of optical model potentials. Those barrier values are in good agreement with the empirical fusion barriers derived by Vaz and Alexander,²⁹ which are $B^p=7.4$ MeV and $B^\alpha=12.2$ MeV for Ru compound nuclei. As the yrast lines and barriers used in PACE2 and CASCADE close to each other, it is suspected that the excess of low-energy particles might originate from a rough description of the level density at low excitation above the yrast line where a consistently large number of alpha particles are emitted in the PACE2 simulation. We note that the level densities for excitation energy below 20 MeV are described carefully in CASCADE, by requiring the matching between the low-energy region which is treated following the Dilg parametrization¹⁹ of the Fermi gas formula and the high-energy region which is described by the same formalism but with parameters from the liquid-drop model.²⁰

As in the case of ^{59}Cu ,^{5,6} we have studied the effects of lowering the yrast line in a spin-dependent way. To this end CASCADE calculations were performed with a third set of input data which includes the fission barrier parameters of set 2 and an *ad hoc* adjusted yrast line shown in Fig. 7.

CASCADE calculations with the set 3 input are compared with the experimental alpha spectra in Fig. 5 and absolute cross sections for p,n alpha emission and fission decay are also shown in Fig. 6 for the ^{58}Ni case. As the lowering of the yrast line causes a spin-dependent enhancement of the level density which changes the phase space available for the alpha emission, the net re-

sult is a decrease of the average energy of the calculated alpha-particle spectra yielding a better production of the experimental data for high as well as for low alpha-particle energy. The worsening of the fit at the lower bombarding energies (135–145 MeV) is caused by a too low yrast line for angular momenta in the range 30–40 \hbar and can be avoided by matching the RLDM to the empirical line in this spin region.

The better agreement obtained, as far as the alpha-particle spectral shape is concerned, corresponds to a drastic decrease in the calculated cross section for the alpha-particle emission, the other decay channels showing smaller changes in cross section. The alpha-particle cross sections from the CASCADE calculations with the set 3 input seem to be too low when compared with the experimental cross section, as shown in Fig. 6.

As discussed by M. Blann,³⁰ the change in nuclear shape should affect also the emission barriers for charged particles at the tip of the elongated nucleus, producing an amplification factor for the cross section. It has been shown that this effect can be accounted for by changing the radii in the optical model potentials. In the present case a small change of the radius (increase of 5%, which means a 3% lowering of the barrier for alpha particles) is enough to restore alpha-particle cross sections of the order of ~ 1.1 b for the $^{32}\text{S}+^{58}\text{Ni}$ reaction at 185 MeV close to the estimates from standard CASCADE (set 2 input) and PACE2. Calculations with this barrier lowering yield shapes of the alpha-particle spectra close to those shown in Fig. 5 (set 3 input).

An important point is the general underestimation of the alpha-particle cross section for bombarding energies in the range 165–185 MeV, clearly due to the opening of the fission channel in model calculations (see in Fig. 6 the differences between CASCADE calculations with set 1 and 2 inputs). Using adjusted RLDM or Sierk fission barriers and transmission coefficients computed from optical model, statistical model calculations are not able to reproduce the experimental data. As an example, the experimental value of 1.5 b for the alpha-particle emission from the $^{32}\text{S}+^{58}\text{Ni}$ at 185 MeV is reproduced only in calculations with transmission coefficients for alpha particles corresponding to a sizeable reduction (10%) of the barrier. The corresponding fission cross section drops to the value 0.2b. Proton and neutron production cross sections are scarcely sensitive to this barrier lowering.

V. CONCLUSIONS

Alpha-particle decay from the $^{90,92,94,96}\text{Ru}$ compound nuclei populated at excitation energies in the range $E_x=60$ –115 MeV and angular momentum values up to $\sim 70\hbar$ have been studied extending the test of statistical models and the search for deformation effects, previously evidenced in lighter systems,^{4–7} in compound nuclei where the fission decay competes with the particle decay at high spin. The quality of agreement between PACE2 calculations and experimental data was found to be strongly dependent on the compound nucleus also at the lower bombarding energies. In case of CASCADE calculations, a good fit to the experimental data is achieved at

lower bombarding energies where nearly spherical compound nuclei are produced, with the only exception of the absolute cross section for the ^{64}Ni target. The dependence of the fit quality on the compound nucleus at low bombarding energies points out that some parametrization of nuclear properties employed or approximations made on the PACE2 calculations are not reliable.

Predictions by PACE2 and CASCADE codes show increasing deviations from the alpha-particle experimental data at the higher bombarding energies and for all the compound nuclei studied. In particular, they show a common excess of energetic alpha particles as evidenced in the case of lighter CN. Those deviations are supposed to be related to the onset of nuclear deformation driven by the spin. The shape of spectra predicted by the two codes differ at low alpha energies: PACE2 exhibits an overproduction of alpha particles below the peak energy, whereas CASCADE underestimates this production as in the case of lighter CN. Large discrepancies between the predicted cross sections are evidenced in the case of p and n decay. These effects are likely to be due to differences in the parametrization of nuclear properties (level densities, binding energies) employed in the two codes.

The discrepancies between standard CASCADE calculations and experimental data are qualitatively smaller than that evidenced for mass $A=50-70$ where the fission channel is less effective in depleting the more deformed states at high spin. This is in agreement with the predictions of the models of rotating nuclei.^{30,31} As in the case of previous works, the discrepancies between the CASCADE predictions and the experimental spectra are removed by modeling the phase space available by chang-

ing the yrast line and the access to this phase space by slightly lowering the emission barrier. The interpretation of the phase space change obtained by lowering the yrast line has been discussed recently for the $^{32}\text{S}+^{27}\text{Al}$ reaction.³² It can be explained in terms of dependence of the level density on the nuclear deformation, as predicted in some theoretical framework or, alternatively, as due to the freezing of the nuclear shape during the particle decay. In the present case, the mean lifetime of the compound system at the maximum excitation is of the order of $1-2 \times 10^{-21}$ s, as computed by the PACE2 code, comparable with neutron emission lifetime in heavy nuclei where pre-fission emission has been evidenced.³³ A contribution to the evidenced phenomena coming from the dynamics of shape relaxation is therefore possible. The need of barrier lowering in statistical model calculations of alpha-particle experimental data is, today, not free from controversies.³ Once modeled the phase space to reproduce the shape of alpha-particle spectra, the resulting predicted cross section values are too low. One way of achieving a larger access to the phase space for the alpha decay is the lowering of the emission barrier. This, in turn, decreases the fission cross section. High quality data on fission-alpha-particle competition are needed to probe the barrier lowering in this mass region.

ACKNOWLEDGMENTS

We thank J. B. Natowitz for a critical reading of the manuscript. This work was supported by Istituto Nazionale di Fisica Nucleare.

*Permanent address: Institute of Nuclear Physics, Cracow, Poland.

¹J. B. Natowitz, Nucl. Phys. **A482**, 171c (1988).

²G. La Rana, D. J. Moses, W. E. Parker, M. Kaplan, D. Logan, R. Lacey, J. M. Alexander, and R. J. Welberry, Phys. Rev. C **35**, 373 (1987); M. Kaplan, D. J. Moses, W. E. Parker, G. La Rana, R. J. Welberry, D. Logan, R. Lacey, J. M. Alexander, D. M. de Castro Rizzo, and P. De Young, in *Proceedings of the Texas A&M Symposium on Hot Nuclei, College Station, 1987*, edited by S. Shlomo, R. P. Schmitt, and J. B. Natowitz (World Scientific, Singapore, 1987), p. 115.

³I. M. Govil, J. R. Huizenga, W. U. Schroder, and J. Toke, Phys. Lett. B **197**, 515 (1987); J. R. Huizenga, A. N. Behkami, I. M. Govil, W. U. Schroder, and J. Toke, University of Rochester Report No. UR-NSRL-342 (1989).

⁴R. K. Choudhury, P. L. Gonthier, K. Hagel, M. N. Namboodiri, J. B. Natowitz, L. Adler, S. Simon, S. Kniffen, and G. Berkowitz, Phys. Lett. **143B**, 74 (1984).

⁵B. Fornal, G. Prete, G. Nebbia, F. Trotti, G. Viesti, D. Fabris, K. Hagel, and J. B. Natowitz, Phys. Rev. C **37**, 2624 (1988).

⁶G. Viesti, B. Fornal, D. Fabris, K. Hagel, J. B. Natowitz, G. Nebbia, G. Prete, and F. Trotti, Phys. Rev. C **38**, 2640 (1988).

⁷Z. Majka, M. E. Brandan, D. Fabris, K. Hagel, A. Menchacha-Rocha, J. B. Natowitz, G. Nebbia, G. Prete, and G. Viesti, Phys. Rev. C **35**, 2125 (1987).

⁸F. Puhlhofer, Nucl. Phys. **A280**, 267 (1977).

⁹Revised version of the code PACE; see A. Gavron, Phys. Rev. C **20**, 230 (1980).

¹⁰A. M. Stefanini *et al.*, Nucl. Phys. **A456**, 509 (1986); H. H. Gutbrod, M. Blann, and W. G. Winn, *ibid.* **213**, 285 (1973).

¹¹W. Scobel, A. Mignerey, M. Blann, and H. H. Gutbrod, Phys. Rev. C **11**, 1701 (1975); W. Scobel, J. Bisplinghoff, M. Blann, A. Mignerey, P. David, J. Ernst, and T. Mayer-Kuckuk, Z. Phys. A **284**, 343 (1978).

¹²W. W. Wilcke, J. R. Birklund, H. J. Wollersheim, A. D. Hoover, J. R. Huizenga, W. U. Schroeder, and L. E. Tubs, At. Data Nucl. Data Tables **25**, 389 (1980).

¹³N. N. Ajitanand, G. La Rana, R. Lacey, D. J. Moses, L. C. Vaz, G. F. Peaslee, D. M. de Castro Rizzo, M. Kaplan, and J. M. Alexander, Phys. Rev. C **34**, 877 (1986), and references therein.

¹⁴W. D. Myers and W. J. Swiatecki, Ark. Fys. **36**, 343 (1967).

¹⁵D. Wilmore and P. E. Hodgson, Nucl. Phys. **55**, 673 (1964); P. E. Hodgson, Annu. Rev. Nucl. Sci. **17**, 1 (1967).

¹⁶F. G. Perey, Phys. Rev. **131**, 745 (1963).

¹⁷J. R. Huizenga and G. Igo, Nucl. Phys. **29**, 462 (1961).

¹⁸D. W. Lang, Nucl. Phys. **77**, 545 (1966).

¹⁹W. Dilg, W. Schantl, H. Vonach, and M. Uhl, Nucl. Phys. **A217**, 269 (1973).

²⁰W. D. Myers and W. J. Swiatecki, Nucl. Phys. **81**, 1 (1966).

²¹F. Plasil, ORNL ALICE, Report ORNL/TM-6054 (1977).

²²A. H. Wapstra and K. Bos, At. Data Nucl. Data Tables **19**,

- 177 (1977).
- ²³A. Gilbert and A. G. W. Cameron, *Can. J. Phys.* **43**, 1446 (1965).
- ²⁴A. J. Sierk, *Phys. Rev. C* **33**, 2039 (1986).
- ²⁵B. Sikora, W. Scobel, M. Beckerman, J. Bisplinghoff, and M. Blann, *Phys. Rev. C* **25**, 1446 (1982).
- ²⁶M. Blann and T. T. Komoto, *Phys. Rev. C* **26**, 472 (1982).
- ²⁷H. J. Krappe, J. R. Nix, and A. J. Sierk, *Phys. Rev.* **20**, 992 (1979).
- ²⁸S. Cohen, F. Plasil and W. Swiatecki, *Ann. Phys. (N.Y.)* **82**, 557 (1974).
- ²⁹L. C. Vaz and J. M. Alexander, *Z. Phys. A* **318**, 231 (1984).
- ³⁰M. Blann, *Phys. Rev. C* **21**, 1770 (1980).
- ³¹M. Blann and T. T. Komoto, *Phys. Rev. C* **24**, 426 (1981).
- ³²B. Fornal, G. Viesti, G. Nebbia, G. Prete, and J. B. Natowitz, *Phys. Rev. C* **40**, 664 (1989).
- ³³D. Hilsher, D. J. Hinde, and H. Rossner, in *Proceedings of the Texas A&M Symposium on Hot Nuclei, College Station*, edited by S. Shlomo, R. P. Schmitt, and J. B. Natowitz (World Scientific, Singapore, 1987), p. 193.